Ionic liquid bmimCl/formamide mixture as the polar phase of nonaqueous microemulsions

Junjie Wei [a,b], Baogen Su [a,*], Ruisi Liang [a], Huabin Xing [a], Zongbi Bao [a], Qiwei Yang [a], Yiwen Yang [a], Qilong Ren [a,*]
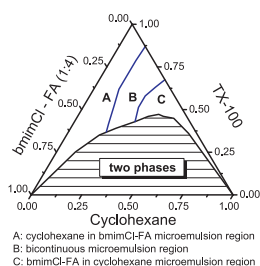
[a] Key Laboratory of Biomass Chemical Engineering of Ministry of Education, Department of Chemical and Biological Engineering, Zhejiang University, Hangzhou 310027, China
[b] Center of Environmental Engineering Technology Assessment, Environmental Protection Bureau, Zhejiang Province, Hangzhou 310012, China

HIGHLIGHTS

- ► Microemulsions with ionic liquid and a nonaqueous polar solvent as the polar phase.
- ► Characterization by means of conductivity, DLS and UV–vis spectroscopy.
- ► Linear increase of the microemulsions droplet size by adding the polar phase.
- ► These nonaqueous microemulsions can dissolve metal salt.

GRAPHICAL ABSTRACT

A: cyclohexane in bmimCl-FA microemulsion region
B: bicontinuous microemulsion region
C: bmimCl-FA in cyclohexane microemulsion region

ARTICLE INFO

ABSTRACT

The solution of ionic liquid (IL) bmimCl and polar organic solvent formamide (FA) were used to form nonaqueous microemulsions in cyclohexane by the aid of surfactant Triton X-100 (TX-100). The phase behavior of the bmimCl–FA/TX-100/cyclohexane system at $25 \pm 0.1\,^\circ$C was studied. Electrical conductivity measurement was used to identify the microstructures of the nonaqueous microemulsions. Based on the phase diagram, the reverse microemulsions containing bmimCl–FA as the internal phase were investigated by the dynamic light scattering (DLS) and UV–vis spectroscopy. The result of DLS experiments confirmed the formation of reverse microemulsions of bmimCl–FA in cyclohexane. The UV–vis studies with methyl orange (MO) and methylene blue (MB) as absorption probes further confirmed the existence of reverse microemulsions. UV–vis studies using $CoCl_2$ as probe also indicated that the reverse microemulsions could dissolve metal salt.

© 2012 Elsevier B.V. All rights reserved.

1. Introduction

Microemulsions are transparent, isotropic and thermodynamically stable mixtures of two immiscible liquids (nonpolar and polar) stabilized by surfactants. The traditional reverse microemulsions use water as the polar component. The surfactant-covered water pools provide a unique microenvironment for reactions and nanoparticle preparation [1,2]. Reverse microemulsions can also be made using some polar organic solvents instead of water. These polar solvents have high dielectric constants and very low solubility in hydrocarbon solvents [3]. The most common polar solvents used for these nonaqueous microemulsions include formamide (FA), dimethylforamide (DMF), and ethylene glycol (EG) [4,5]. These waterless microemulsions have attracted much interest and have been widely applied in many fields.

Ionic liquids (ILs), which are typically composed of organic cations and organic/inorganic anions, are receiving much attention as neoteric solvents. They have many attractive properties, such as negligible vapor pressure, a wide electrochemical window, and high thermal stability. Particularly, the properties of ILs

---

* Corresponding authors. Tel.: +86 571 8795 2773; fax: +86 571 8795 2773.
E-mail addresses: subg@zju.edu.cn (B. Su), renql@zju.edu.cn (Q. Ren).

can be tuned by altering either the cation or the anion [6]. In the past decade, ILs have been used in various chemical applications including chemical reactions, separations, material preparation, and electrochemical applications. The unique properties of ILs are favored for increasing the efficiency of reaction and separation, and controllability of material preparation [7–10].

ILs can also play an important role in microemulsions [11–13]. Recently, using ILs instead of water to prepare nonaqueous microemulsions is an active subject. These new nonaqueous microemulsions expand the potential use of ILs in micro-heterogeneous systems as reaction or separation media [14]. Han and co-workers discovered that hydrophilic IL 1-butyl-3-methylimidazolium tetrafluoroborate ($bmimBF_4$) can substitute for water and act as polar nanosized droplets dispersed in cyclo-hexane with the surfactant Triton X-100 (TX-100) [15]. Eastoe et al. investigated the same microemulsions by small-angle neutron scattering (SANS), which showed a regular increase in droplet volume as the micelles were progressively swollen with added $bmimBF_4$, a behavior consistent with classic water-in-oil (W/O) microemulsions [14]. Zheng and co-workers found that $bmimBF_4$ can form nonaqueous microemulsions with benzene [16], toluene [17], *p*-xylene [18] or triethylamine [19] also using TX-100 as surfactant. The structure and properties of these microemulsions were further investigated using various methods by many groups [20–25]. Additionally, the hydrophobic ILs, such as 1-butyl-3-methylimidazolium hexafluorophosphate ($bmimPF_6$) can also form nonaqueous microemulsions [26–30]. The IL microemulsions have potential application in the production and processing of semiconductors, nanomaterials, enzyme-catalyzed reactions, and extraction [21]. Compared to traditional microemulsions, they have shown various advantages, especially in the preparation of nano-structures [31–33].

However, in current studies, the ILs used are room-temperature ILs [34], which possess relatively small viscosity. As we known, ILs are often extraordinarily viscous or even solid near room temperature [35]. Take the chloride anion-based ILs as an example, they are solid near room temperature and should be diluted with traditional molecular solvents in some applications [9,36]. Therefore, the broader use of ILs to form nonaqueous microemulsions is limited. Using the mixture of an IL and nonaqueous polar solvents instead of pure ILs may be a prospective approach to this problem. The addition of polar solvents can significantly reduce the viscosity of the IL phase [37]. Moreover, this type of nonaqueous microemulsions may have advantages in tuning the properties of the polar microenvironment as the chemical properties of the solution of IL and polar solvent can be adjusted by altering the IL or polar solvent [38].

The present work investigates the formation of nonaqueous microemulsions containing the mixture of IL and polar solvent as the polar phase. For this purpose, a chloride anion-based IL 1-butyl-3-methylimidazolium chloride (bmimCl) was chosen as a model IL. Formamide, which has very low solubility in hydrocarbon solvents [39], was chosen as the polar solvent. Then, in this work, these nonaqueous microemulsions were prepared and characterized using different techniques, including electrical conductivity, dynamic light scattering (DLS) and UV–vis spectroscopy.

2. Experimental

2.1. Materials

TX-100 was obtained from Sigma–Aldrich and dried under vacuum at 80 °C for 4 h before use. The IL bmimCl (purity > 99%) was provided by Lanzhou GreenChem ILS, LICP, CAS (China). Formamide (purity > 99%) was purchased from Lingfeng Co., Ltd. (Shanghai,

China). Cyclohexane (purity > 99.5%) and methyl orange (MO) were purchased from Sinopharm Chemical Reagent Co., Ltd. (Shanghai, China). Methylene blue (MB) was produced by Dongsheng Chemical Reagents Co. (Zhejiang, China). $CoCl_2$ was a product of Jingchun Reagent Co., Ltd. (Shanghai, China).

2.2. Apparatus and procedures

The phase diagram of the system was determined by direct visual observation at 25 ± 0.1 °C. In a typical experiment, bmimCl–FA and cyclohexane were added into a thermostated glass vessel; the sample was then agitated. After thermal equilibrium, the sample was then titrated with TX-100 until the hazy and milky liquid solution became transparent, which was indicative of the formation of the single phase. The corresponding composition of the solution was remarked as the phase boundary. The bmimCl–FA was a solution of IL bmimCl in FA with a fixed bmimCl to FA molar ratio (1:4), which was regarded as pseudo one component.

Conductivity measurement was performed with a DDS-11 A conductivity meter (Shanghai Precision & Scientific Instrument Co., Ltd.). In the experiment, the desired amounts of bmimCl–FA and TX-100 were mixed in a thermostated glass vessel at the temperature of 25 ± 0.1 °C. Then a certain amount of cyclohexane was added. After thorough mixing and thermal equilibrium, the electrical conductivity was recorded. The cyclohexane was successively added to the mixture with a transferpette (Brand Co., Ltd., Germany) until the transparent liquid solution became turbid. The conductivity was measured after each addition of cyclohexane.

The diameters of the microemulsion droplets were determined by dynamic light scattering (DLS, Zetasizer Nano ZS, Malvern Instruments, UK) with a laser light wavelength of 633 nm and a scattering angle at 173°. The sample was filtered through 0.45 μm millipore membrane filter to remove possible dusts prior to measurement. All measurements were conducted at 25 °C.

The UV–vis spectra were performed on a Shimadzu UV-2550 spectrophotometer at 25 ± 0.1 °C. The path length of the quartz cell used in this experiment was 1 cm. The solutions were prepared in advance and then added to the quartz cell.

3. Results and discussion

3.1. Phase diagram and microregions of the microemulsions

The phase diagram of the bmimCl–FA/TX-100/cyclohexane system at 25 ± 0.1 °C is illustrated in Fig. 1. The shadow area of the diagram marked "two phases" is a turbid region. Above the phase separation boundary curve, the system exists as a single phase. Generally, the single phase region of microemulsions can be divided into different microregions, such as water (or polar solvent)-in-oil microemulsions region, bicontinuous microemulsions region and oil-in-water (or polar solvent) microemulsions region [26]. In this work, the microregions were identified by electrical conductivity measurement, which was frequently used to investigate the structure and structural changes in aqueous and nonaqueous microemulsions [26]. Thus the electrical conductivity as a function of cyclohexane weight fraction at different fixed weight ratios of bmimCl–FA to TX-100 (1:9, 2:8, 3:7, 4:6, 5:5) was investigated. The test samples are shown in Fig. 1 (lines a–e).

Two typical curves of conductivity versus cyclohexane concentration are shown in Fig. 2. As an example, Fig. 2a illustrates how to distinguish the microregions of the microemulsions on the basis of the conductivity data. The initial conductivity increases with the increase of the content of cyclohexane, due to the successive increase of conductive microemulsion droplets, which indicates the formation of cyclohexane in bmimCl–FA microemulsions. After

84

J. Wei et al. / Colloids and Surfaces A: Physicochem. Eng. Aspects 414 (2012) 82–87
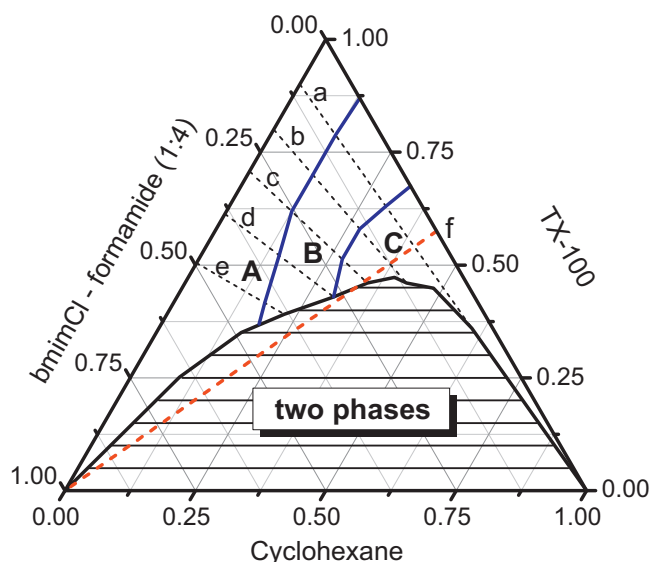
Fig. 1. Phase diagram of the bmimCl–FA (1:4)/TX-100/cyclohexane system at 25 ± 0.1 °C. A–C are cyclohexane in bmimCl–FA, bicontinuous, and bmimCl–FA in cyclohexane regions, respectively. The lines a–e are chosen for the electric conductivity measurement. For line f, the initial TX-100 weight fraction is 0.575.
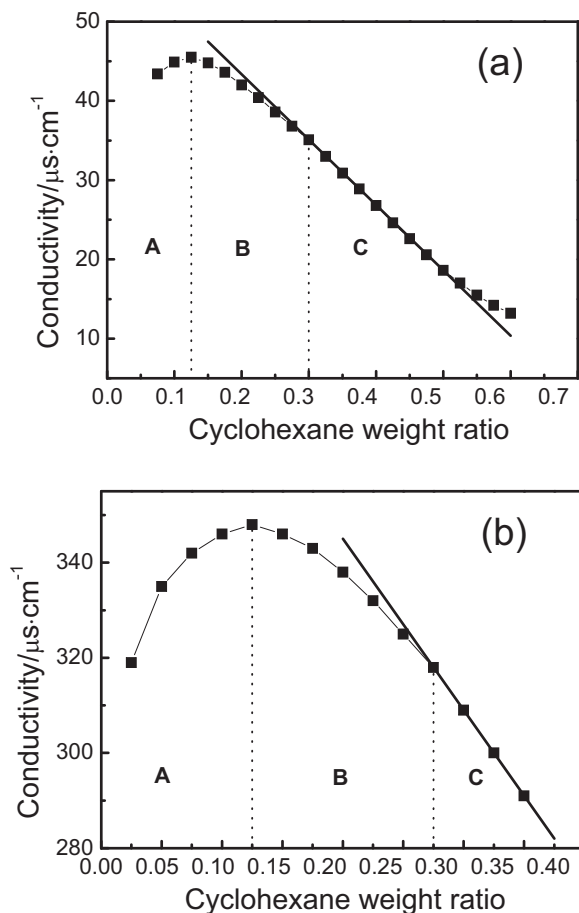

Fig. 2. Electrical conductivity of the microemulsion solutions as a function of cyclohexane content at 25 ± 0.1 °C. A–C are cyclohexane in bmimCl–FA, bicontinuous, and bmimCl–FA in cyclohexane regions, respectively. The weight fractions of bmimCl–FA (1:4) to TX-100 are 1:9 (a) and 3:7 (b).

reaching a maximum, the conductivity decreases nonlinearly. It reveals that the bicontinuous microemulsions are formed, which can be ascribed to the gradual growth and interconnection of the cyclohexane in bmimCl–FA microemulsion droplets. A further addition of cyclohexane leads to a linear decrease of conductivity. It can be interpreted as a result of the formation of reverse microemulsions of bmimCl–FA in cyclohexane resulting from the partial fusion of clustered inverse microdroplets. The final nonlinear decrease of conductivity corresponds to the existence of a percolation phenomenon, suggesting inverse droplet aggregation appeared [17,27]. As mentioned above, Fig. 2a illustrates the presence of three different types of microstructure: cyclohexane in bmimCl–FA, bicontinuous, and bmimCl–FA in cyclohexane microemulsions. Using this method, three types of microregions in the single phase microemulsions were determined (Fig. 1). Based on the phase diagram, it can be observed that the reverse microemulsions with the solution of bmimCl and FA as the polar internal phase can be formed. As proposed by Gao et al. [18], the interaction between the electronegative oxygen atoms of the oxyethylene (OE) units of TX-100 and the electropositive imidazolium ring of IL may be the driving force for the solubilization of bmimCl–FA into the core of the TX-100 aggregates, which may be the mechanism of the formation of the nonaqueous microemulsions. In order to demonstrate the formation of these reverse microemulsions, further studies were performed.

3.2. DLS studies

The DLS method was used to investigate the size of the reverse microemulsions. Typical size and size distributions of microemulsions of bmimCl–FA in cyclohexane (along line f in Fig. 1) obtained by DLS method are presented in Fig. 3, wherein the weight ratio of TX-100 to cyclohexane is 0.575:0.425, and the bmimCl–FA to TX-100 mole ratios (R) are 0.36, 0.62, 0.98, 1.32, 1.77 and 2.18, respectively. Here, the molecular weight of bmimCl–FA (1:4) is defined as $Mw_{(bmimCl-FA)} = 0.2 \times Mw_{(bmimCl)} + 0.8 \times Mw_{(FA)}$. It is observed that the droplet sizes of microemulsions increase from 14.6 to 29.7 nm with the increase of R value from 0.36 to 2.18. This indicates that the micelles are swollen by bmimCl–FA. The result presented in Fig. 4 indicates a linear correlation between the droplet size and R value. This behavior is consistent with classic W/O microemulsions and also similar to some IL microemulsions reported by other researchers [15,18,40]. The results of DLS experiments confirmed the formation of reverse microemulsions, which contained bmimCl and FA in the internal polar pool.
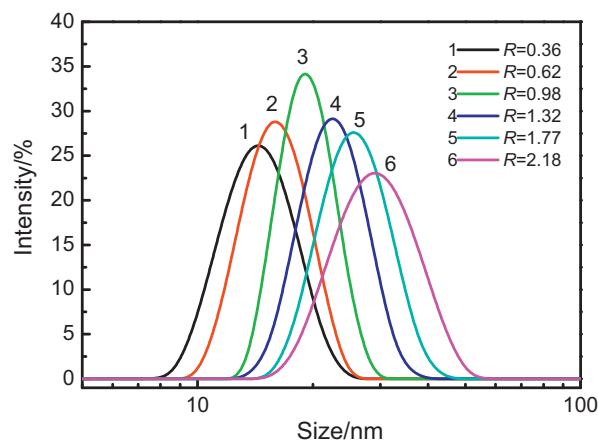
Fig. 3. Size and size distribution of the microemulsion droplets of bmimCl–FA in cyclohexane at 25 °C (along line f in Fig. 1) with different R values.
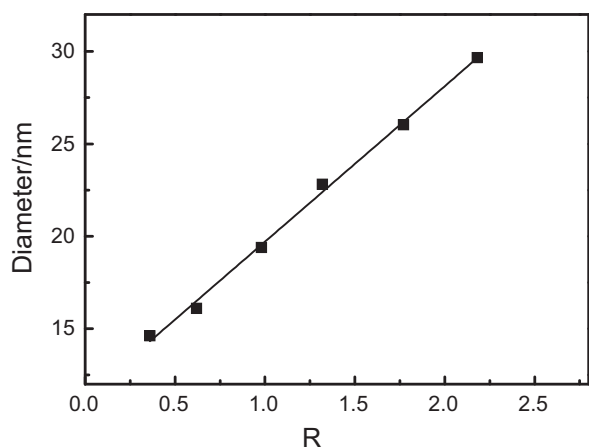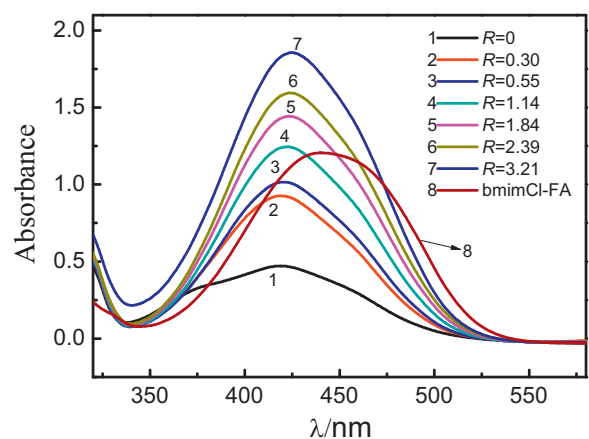
Fig. 4. Dependence of droplet size on bmimCl–FA to TX-100 molar ratio (*R*) for the microemulsions of bmimCl–FA in cyclohexane at 25 °C.

Fig. 6. Absorption spectra of MB in microemulsions of bmimCl–FA in cyclohexane at 25 °C (along line f in Fig. 1) with different *R* values and in bmimCl–FA (1:4) solution. Probe concentrations: 1.9×10^{-5} M (1–7) and 1.3×10^{-5} M (8).
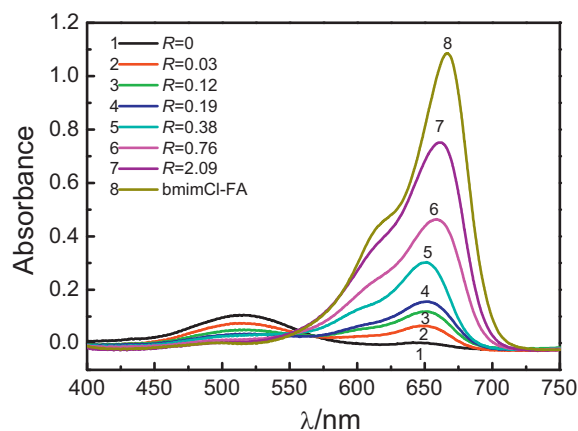
3.3. UV–vis studies

UV–vis spectroscopy was used to characterize the environment of microemulsions of bmimCl–FA in cyclohexane. MO is often used as a probe to study the polarity of the polar domains in microemulsions [41,42]. The shift in the absorbance maximum (λ_{max}) of MO is a sensitive measurement of the local environment. As a red-shift indicator, the λ_{max} of MO shifts to longer wavelength as the media polarity increases [43]. Fig. 5 shows the effect of the successive addition of bmimCl–FA on the absorption spectra of MO in the TX-100/cyclohexane binary system. As expected, the λ_{max} of the MO increases from 418.0 to 424.8 nm with the *R* value from 0 to 3.21. The red shift in the λ_{max} value indicates that the polarity of the microdomain increases, but the polarity of the microdomain is still weaker than that of the bulk bmimCl–FA ($\lambda_{max} = 440$ nm, Fig. 5).

The microenvironment of microemulsions of bmimCl–FA in cyclohexane was also investigated using MB as absorption probe. TX-100 has a strong interaction with the cationic dye MB [44]. The complexation between TX-100 and MB in the reverse micelles is sensitive to its interaction with its local environment, which leads to that MB is an effective absorption probe to study the microenvironment in nonionic reverse microemulsions [45].

The effect of the successive addition of bmimCl–FA on the absorption spectra of MB in the TX-100/cyclohexane binary system

Fig. 5. Absorption spectra of MO in microemulsions of bmimCl–FA in cyclohexane at 25 °C (along line f in Fig. 1) with different *R* values and in bmimCl–FA (1:4) solution. Probe concentrations from 1 to 8: 3.0×10^{-5}, 3.6×10^{-5}, 4.1×10^{-5}, 5.0×10^{-5}, 5.9×10^{-5}, 6.6×10^{-5}, 7.7×10^{-5} and 4.4×10^{-5} M.

was investigated. As shown in Fig. 6, the λ_{max} of the MB in the TX-100/cyclohexane mixture is 515 nm, which is remarkably different from that of MB in bmimCl–FA ($\lambda_{max} = 667$ nm). The formation of 1:1 complex between MB and TX-100 leads to a remarkable blue shift of MB absorption band [44]. As described in previous studies [16,21], the absorption band at 515 nm can be ascribed to the 1:1 MB·TX-100 complex. However, this absorption band begins to disappear gradually with the successive addition of bmimCl–FA. Meanwhile, a new absorption band with a continuous increase in intensity at the higher wavelength region was observed. This phenomenon can be interpreted as follows. As the bmimCl–FA added, the polar pool begins to form. Because the MB favors the bmimCl–FA solution, more and more MB molecules are dissolved into the polar pool. Thus there is a continuous increase in intensity at the higher wavelength region. This in turn decreases the amount of the MB·TX-100 complex, which results in the gradual decrease of the absorption band at 515 nm. Besides, with the addition of bmimCl–FA, the λ_{max} of the new absorption band at the higher wavelength region increases until close to that of MB in bmimCl–FA ($\lambda_{max} = 667$ nm). This may due to the different polarity of the microemulsions. However, MB is not a suitable micropolarity probe, since the absorption spectra of MB does not show regular polarity dependence [45].

CoCl$_2$ was chosen as a model metal salt to study the solubilization of metal salts in this nonaqueous microemulsions because of the obvious color and absorption characteristics of the Co^{2+} [21,46]. A series of microemulsions of bmimCl–FA in cyclohexane were prepared with a fixed TX-100 to cyclohexane weight ratio (0.575:0.425), and a fixed bmimCl–FA to surfactant molar ratio (*R* = 1.86), but with different CoCl$_2$ concentrations. The UV–vis spectra of CoCl$_2$ in the microemulsions are presented in Fig. 7. It can be seen from Fig. 7 that there are three characteristic absorption peaks of CoCl$_2$, which is the same as that in bmimCl–FA solution. This reveals that CoCl$_2$ is solubilized in an environment that is similar to bmimCl–FA solution. Thus, the formation of microemulsions of bmimCl–FA in cyclohexane is further confirmed. In addition, as shown in Fig. 8, the absorbance of CoCl$_2$ at the λ_{max} (696 nm) increases linearly with CoCl$_2$ concentration. The result is in agreement with the Lambert–Beer law. From this experiment, it is reasonable to consider that the nonaqueous microemulsions could dissolve metal salts.

The UV–vis studies further confirm the formation of microemulsions of bmimCl–FA in cyclohexane. This type of nonaqueous reverse microemulsions may have advantages in tuning the properties of the polar microenvironment by altering the IL or polar
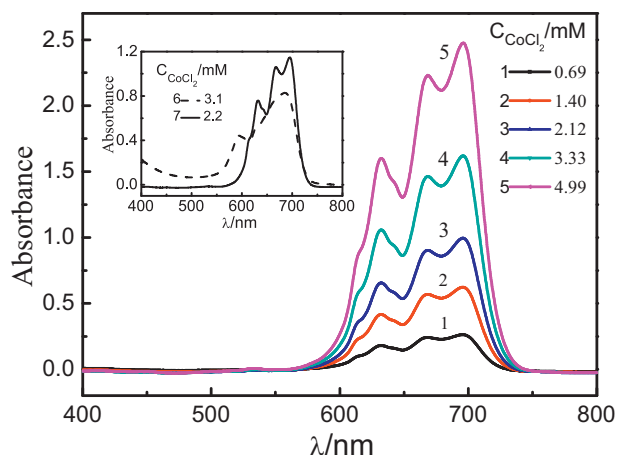
Fig. 7. Absorption spectra of $CoCl_2$ in microemulsions of bmimCl–FA in cyclohexane at $R = 1.86$ with different $CoCl_2$ concentrations at 25 °C. Inset shows the absorption spectra of $CoCl_2$ in TX-100/cyclohexane (0.575/0.425 by weight) solution (6) and the bmimCl–FA (1:4) solution (7) at 25 °C.
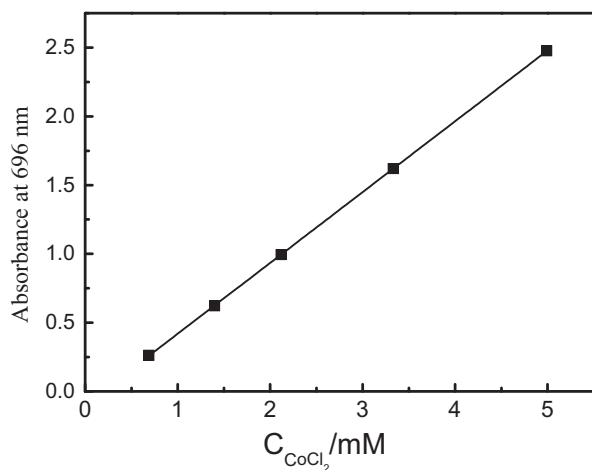
Fig. 8. The maximum absorbance intensity of $CoCl_2$ in the microemulsions with $CoCl_2$ concentration.

solvent, especially the IL because of their various types. As a result, this type of nonaqueous microemulsions may have potential applications in catalysis, nanomaterials preparation, and separation.

4. Conclusion

Nonaqueous microemulsions composed of the solution of bmimCl and FA as polar phase, surfactant TX-100, and cyclohexane as the oil phase were prepared. The phase behavior of this system was investigated. The bmimCl–FA in cyclohexane, bicontinuous, and cyclohexane in bmimCl–FA microregions of the nonaqueous microemulsions were identified by electrical conductivity measurements. DLS studies reveal that the droplet sizes of reverse microemulsions of bmimCl–FA in cyclohexane are increased linear with the increase of bmimCl–FA content. The polarity of the polar domains in these reverse microemulsions was investigated by UV–vis spectroscopy using MO and MB as absorption probes. It also shows that metal salt $CoCl_2$ can be dissolved in these nonaqueous reverse microemulsions. These nonaqueous reverse microemulsions with the solution of IL and polar organic solvent as the internal phase may have advantages in tuning the properties of the internal microenvironment by altering the IL or polar solvent.

References

[1] I. Capek, Preparation of metal nanoparticles in water-in-oil (w/o) microemulsions, Adv. Colloid Interface Sci. 110 (2004) 49–74.
[2] M.A. López-Quintela, C. Tojo, M.C. Blanco, L. García-Río, J.R. Leis, Microemulsion dynamics and reactions in microemulsions, Curr. Opin. Colloid Interface Sci. 9 (2004) 264–278.
[3] A. Martino, E.W. Kaler, Phase behavior and microstructure of nonaqueous microemulsions, J. Phys. Chem. 94 (1990) 1627–1631.
[4] S. Ray, S.P. Moulik, Dynamics and thermodynamics of aerosol OT-aided nonaqueous microemulsions, Langmuir 10 (1994) 2511–2515.
[5] R.D. Falcone, J.J. Silber, N.M. Correa, What are the factors that control nonaqueous/AOT/n-heptane reverse micelle sizes? A dynamic light scattering study, Phys. Chem. Chem. Phys. 11 (2009) 11096–11100.
[6] J.L. Anderson, J. Ding, T. Welton, D.W. Armstrong, Characterizing ionic liquids on the basis of multiple solvation interactions, J. Am. Chem. Soc. 124 (2002) 14247–14254.
[7] T. Welton, Room-temperature ionic liquids. Solvents for synthesis and catalysis, Chem. Rev. 99 (1999) 2071–2083.
[8] N.V. Plechkova, K.R. Seddon, Applications of ionic liquids in the chemical industry, Chem. Soc. Rev. 37 (2008) 123–150.
[9] Q.W. Yang, H.B. Xing, Y.F. Cao, B.G. Su, Y.W. Yang, Q.L. Ren, Selective separation of tocopherol homologues by liquid–liquid extraction using ionic liquids, Ind. Eng. Chem. Res. 48 (2009) 6417–6422.
[10] K.L. Ding, Z.J. Miao, B.J. Hu, G.M. An, Z.Y. Sun, B.X. Han, Z.M. Liu, Study on the anatase to rutile phase transformation and controlled synthesis of rutile nanocrystals with the assistance of ionic liquid, Langmuir 26 (2010) 10294–10302.
[11] O. Rojas, J. Koetz, S. Kosmella, B. Tiersch, P. Wacker, M. Kramer, Structural studies of ionic liquid-modified microemulsions, J. Colloid Interface Sci. 333 (2009) 782–790.
[12] J.J. Wei, B.G. Su, J.X. Yang, H.B. Xing, Z.B. Bao, Y.W. Yang, Q.L. Ren, Water solubilization capacity and volume-induced percolation of sodium bis(2-ethylhexyl)sulfosuccinate microemulsions in the presence of 1-alkyl-3-methylimidazolium chloride ionic liquids, J. Chem. Eng. Data 56 (2011) 3698–3702.
[13] J.J. Wei, B.G. Su, H.B. Xing, Z.B. Bao, Y.W. Yang, Q.L. Ren, Effect of ionic liquids on temperature-induced percolation behavior of AOT microemulsions, Colloids Surf. A 396 (2012) 213–218.
[14] J. Eastoe, S. Gold, S.E. Rogers, A. Paul, T. Welton, R.K. Heenan, I. Grillo, Ionic liquid-in-oil microemulsions, J. Am. Chem. Soc. 127 (2005) 7302–7303.
[15] H.X. Gao, J.C. Li, B.X. Han, W.N. Chen, J.L. Zhang, R. Zhang, D.D. Yan, Microemulsions with ionic liquid polar domains, Phys. Chem. Chem. Phys. 6 (2004) 2914–2916.
[16] Y.A. Gao, N. Li, L.Q. Zheng, X.Y. Zhao, J. Zhang, Q. Cao, M.W. Zhao, Z. Li, G.Y. Zhang, The effect of water on the microstructure of 1-butyl-3-methylimidazolium tetrafluoroborate/TX-100/benzene ionic liquid microemulsions, Chem. Eur. J. 13 (2007) 2661–2670.
[17] Y.A. Gao, S.Q. Wang, L.Q. Zheng, S.B. Han, X. Zhang, D.M. Lu, L. Yu, Y.Q. Ji, G.Y. Zhang, Microregion detection of ionic liquid microemulsions, J. Colloid Interface Sci. 301 (2006) 612–616.
[18] Y.A. Gao, J. Zhang, H.Y. Xu, X.Y. Zhao, L.Q. Zheng, X.W. Li, L. Yu, Structural studies of 1-butyl-3-methylimidazolium tetrafluoroborate/TX-100/p-xylene ionic liquid microemulsions, ChemPhysChem 7 (2006) 1554–1561.
[19] N. Li, Q. Cao, Y.A. Gao, J. Zhang, L.Q. Zheng, X.T. Bai, B. Dong, Z. Li, M.W. Zhao, L. Yu, States of water located in the continuous organic phase of 1-butyl-3-methylimidazolium tetrafluoroborate/Triton X-100/triethylamine reverse microemulsions, ChemPhysChem 8 (2007) 2211–2217.
[20] D. Chakrabarty, D. Seth, A. Chakraborty, N. Sarkar, Dynamics of solvation and rotational relaxation of coumarin 153 in ionic liquid confined nanometer-sized microemulsions, J. Phys. Chem. B 109 (2005) 5753–5758.
[21] N. Li, Y.A. Gao, L.Q. Zheng, J. Zhang, L. Yu, X.W. Li, Studies on the micropolarities of bmimBF$_4$/TX-100/toluene ionic liquid microemulsions and their behaviors characterized by UV–visible spectroscopy, Langmuir 23 (2007) 1091–1097.
[22] N. Li, S.H. Zhang, L.Q. Zheng, Y.A. Gao, L. Yu, Second virial coefficient of bmimBF$_4$/Triton X-100/cyclohexane ionic liquid microemulsion as investigated by microcalorimetry, Langmuir 24 (2008) 2973–2976.
[23] Y.A. Gao, L. Hilfert, A. Voigt, K. Sundmachert, Decrease of droplet size of the reverse microemulsion 1-butyl-3-methylimidazolium tetrafluoroborate/Triton X-100/cyclohexane by addition of water, J. Phys. Chem. B 112 (2008) 3711–3719.
[24] Y.A. Gao, N. Li, L. Hilfert, S.H. Zhang, L.Q. Zheng, L. Yu, Temperature-induced microstructural changes in ionic liquid-based microemulsions, Langmuir 25 (2009) 1360–1365.

[25] O. Rojas, B. Tiersch, S. Frasca, U. Wollenberger, J. Koetz, A new type of microemulsion consisting of two halogen-free ionic liquids and one oil component, Colloids Surf. A 369 (2010) 82–87.

[26] J.C. Li, J.L. Zhang, H.X. Gao, B.X. Han, L. Gao, Nonaqueous microemulsion-containing ionic liquid [bmim][PF$_6$] as polar microenvironment, Colloid Polym. Sci. 283 (2005) 1371–1375.

[27] Y.J. Zheng, W.M.J. Eli, G. Li, FTIR study of Tween80/1-butyl-3-methylimidazolium hexafluorophosphate/toluene microemulsions, Colloid Polym. Sci. 287 (2009) 871–876.

[28] F. Gayet, C. El Kalamouni, P. Lavedan, J.D. Marty, A. Brûlet, N. Lauth-de Viguerie, Ionic liquid/oil microemulsions as chemical nanoreactors, Langmuir 25 (2009) 9741–9750.

[29] R.D. Falcone, N.M. Correa, J.J. Silber, On the formation of new reverse micelles: a comparative study of benzene/surfactants/ionic liquids systems using UV–visible absorption spectroscopy and dynamic light scattering, Langmuir 25 (2009) 10426–10429.

[30] R. Pramanik, S. Sarkar, C. Ghatak, V.G. Rao, P. Setua, N. Sarkar, Microemulsions with surfactant TX100, cyclohexane, and an ionic liquid investigated by conductance, DLS, FTIR measurements, and study of solvent and rotational relaxation within this microemulsion, J. Phys. Chem. B 114 (2010) 7579–7586.

[31] F. Yan, J. Texter, Surfactant ionic liquid-based microemulsions for polymerization, Chem. Commun. (2006) 2696–2698.

[32] Z.H. Li, H.L. Zhang, J.M. Du, B.X. Han, J.Q. Wang, Preparation of silica micro-rods with nano-sized pores in ionic liquid microemulsions, Colloids Surf. A 286 (2006) 117–120.

[33] M.W. Zhao, L.Q. Zheng, X.T. Bai, N. Li, L. Yu, Fabrication of silica nanoparticles and hollow spheres using ionic liquid microemulsion droplets as templates, Colloids Surf. A 346 (2009) 229–236.

[34] Z.H. Hu, C.J. Margulis, Room-temperature ionic liquids: slow dynamics, viscosity, and the red edge effect, Acc. Chem. Res. 40 (2007) 1097–1105.

[35] K.N. Marsh, J.A. Boxall, R. Lichtenthaler, Room temperature ionic liquids and their mixtures – a review, Fluid Phase Equilib. 219 (2004) 93–98.

[36] Q.W. Yang, H. Zhang, B.G. Su, Y.W. Yang, Q.L. Ren, H.B. Xing, Volumetric properties of binary mixtures of 1-butyl-3-methylimidazolium chloride + water or hydrophilic solvents at different temperatures, J. Chem. Eng. Data 55 (2010) 1750–1754.

[37] A.L. Zhu, J.J. Wang, L.J. Han, M.H. Fan, Measurements and correlation of viscosities and conductivities for the mixtures of imidazolium ionic liquids with molecular solutes, Chem. Eng. J. 147 (2009) 27–35.

[38] B.R. Mellein, S.N.V.K. Aki, R.L. Ladewski, J.F. Brennecke, Solvatochromic studies of ionic liquid/organic mixtures, J. Phys. Chem. B 111 (2007) 131–138.

[39] R.E. Riter, J.R. Kimmel, E.P. Undiks, N.E. Levinger, Novel reverse micelles partitioning nonaqueous polar solvents in a hydrocarbon continuous phase, J. Phys. Chem. B 101 (1997) 8292–8297.

[40] A. Safavi, N. Maleki, F. Farjami, Phase behavior and characterization of ionic liquids based microemulsions, Colloids Surf. A 355 (2010) 61–66.

[41] B.G. Su, W. Chen, H.B. Xing, Y.W. Yang, Q.L. Ren, Phase behavior and micropolarity of ammonium carboxylate perfluoropolyether reverse micelles in supercritical carbon dioxide, J. Chem. Eng. Data 54 (2009) 1884–1888.

[42] J.J. Wei, B.G. Su, H.B. Xing, H. Zhang, Q.W. Yang, Q.L. Ren, Progress in supercritical CO$_2$ microemulsions with hydrocarbon surfactants, Prog. Chem. 21 (2009) 1141–1148.

[43] D.M. Zhu, Z.A. Schelly, Investigation of the microenvironment in Triton X-100 reverse micelles using methyl orange and methylene blue as absorption probes, Langmuir 8 (1992) 48–50.

[44] D. Pramanick, D. Mukherjee, Molecular interaction of methylene blue with Triton X-100 in reverse micellar media, J. Colloid Interface Sci. 157 (1993) 131–134.

[45] L.M. Qi, J.M. Ma, Investigation of the microenvironment in nonionic reverse micelles using methyl orange and methylene blue as absorption probes, J. Colloid Interface Sci. 197 (1998) 36–42.

[46] K. Behera, N.I. Malek, S. Pandey, Visual evidence for formation of water-in-ionic liquid microemulsions, ChemPhysChem 10 (2009) 3204–3208.